Universiteit Leiden
The Netherlands

Progression of non-obstructive coronary plaque: a practical CCTA-based risk score from the PARADIGM registry

Pontone, G.; Rossi, A.; Baggiano, A.; Andreini, D.; Conte, E.; Fusini, L.; ... ; Chang, H.J.

Citation

Pontone, G., Rossi, A., Baggiano, A., Andreini, D., Conte, E., Fusini, L., ... Chang, H. J. (2023). Progression of non-obstructive coronary plaque: a practical CCTA-based risk score from the PARADIGM registry. *European Radiology*, *34*, 2665-2676. doi:10.1007/s00330-023-09880-x

Version:	Publisher's Version
License:	Creative Commons CC BY 4.0 license
Downloaded from:	https://hdl.handle.net/1887/3762054

Note: To cite this publication please use the final published version (if applicable).

European Radiology (2024) 34:2665–2676
https://doi.org/10.1007/s00330-023-09880-x

European Radiology
EUROPEAN SOCIETY OF RADIOLOGY

CARDIAC

Progression of non-obstructive coronary plaque: a practical CCTA-based risk score from the PARADIGM registry

Gianluca Pontone[1,2] · Alexia Rossi[3,4] · Andrea Baggiano[1] · Daniele Andreini[1,5] · Edoardo Conte[1] · Laura Fusini[1] · Chaterine Gebhard[3,4] · Mark G. Rabbat[6] · Andrea Guaricci[7] · Marco Guglielmo[1] · Giuseppe Muscogiuri[1] · Saima Mushtaq[1] · Mouaz H. Al-Mallah[8] · Daniel S. Berman[9] · Matthew J. Budoff[10] · Filippo Cademartiri[11] · Kavitha Chinnaiyan[12] · Jung Hyun Choi[13] · Eun Ju Chun[14] · Pedro de Araújo Gonçalves[15,16] · Ilan Gottlieb[17] · Martin Hadamitzky[18] · Yong Jin Kim[19] · Byoung Kwon Lee[20] · Sang-Eun Lee[21,22] · Erica Maffei[23] · Hugo Marques[15] · Habib Samady[24] · Sanghoon Shin[21] · Ji Min Sung[22,25] · Alexander van Rosendael[26] · Renu Virmani[27] · Jeroen J. Bax[28,29] · Jonathon A. Leipsic[30] · Fay Y. Lin[26] · James K. Min[31] · Jagat Narula[32] · Leslee J. Shaw[26] · Hyuk-Jae Chang[22,25]

Received: 18 September 2022 / Revised: 27 March 2023 / Accepted: 14 April 2023 / Published online: 26 September 2023
© The Author(s), under exclusive licence to European Society of Radiology 2023

Abstract

Objectives No clear recommendations are endorsed by the different scientific societies on the clinical use of repeat coronary computed tomography angiography (CCTA) in patients with non-obstructive coronary artery disease (CAD). This study aimed to develop and validate a practical CCTA risk score to predict medium-term disease progression in patients at a low-to-intermediate probability of CAD.

Methods Patients were part of the Progression of AtheRosclerotic PlAque Determined by Computed Tomographic Angiography Imaging (PARADIGM) registry. Specifically, 370 (derivation cohort) and 219 (validation cohort) patients with two repeat, clinically indicated CCTA scans, non-obstructive CAD, and absence of high-risk plaque (≥ 2 high-risk features) at baseline CCTA were included. Disease progression was defined as the new occurrence of ≥ 50% stenosis and/or high-risk plaque at follow-up CCTA.

Results In the derivation cohort, 104 (28%) patients experienced disease progression. The median time interval between the two CCTAs was 3.3 years (2.7–4.8). Odds ratios for disease progression derived from multivariable logistic regression were as follows: 4.59 (95% confidence interval: 1.69–12.48) for the number of plaques with spotty calcification, 3.73 (1.46–9.52) for the number of plaques with low attenuation component, 2.71 (1.62–4.50) for 25–49% stenosis severity, 1.47 (1.17–1.84) for the number of bifurcation plaques, and 1.21 (1.02–1.42) for the time between the two CCTAs. The *C*-statistics of the model were 0.732 (0.676–0.788) and 0.668 (0.583–0.752) in the derivation and validation cohorts, respectively.

Conclusions The new CCTA-based risk score is a simple and practical tool that can predict mid-term CAD progression in patients with known non-obstructive CAD.

Clinical relevance statement The clinical implementation of this new CCTA-based risk score can help promote the management of patients with non-obstructive coronary disease in terms of timing of imaging follow-up and therapeutic strategies.

Key Points

- *No recommendations are available on the use of repeat CCTA in patients with non-obstructive CAD.*
- *This new CCTA score predicts mid-term CAD progression in patients with non-obstructive stenosis at baseline.*
- *This new CCTA score can help guide the clinical management of patients with non-obstructive CAD.*

Keywords Computed tomography angiography · Coronary artery disease · Disease progression

Gianluca Pontone and Alexia Rossi provided equal contribution as first authors.

✉ Gianluca Pontone
gianluca.pontone@ccfm.it
Extended author information available on the last page of the article

Abbreviations

CABG	Coronary artery bypass graft
CAC	Coronary artery calcium
CAD	Coronary artery disease
CCTA	Coronary computed tomography angiography

DLP	Dose-length product
HRP	High-risk plaque
HU	Hounsfield unit
LAD	Left anterior descending coronary artery
LM	Left main coronary artery
PARADIGM	Progression of AtheRosclerotic PlAque Determined by Computed Tomographic Angiography Imaging
PCI	Percutaneous coronary intervention
PROMISE	Prospective Multicenter Imaging Study for Evaluation of Chest Pain
SCCT	Society of Cardiovascular Computed Tomography
SCOT-HEART	Scottish Computed Tomography of the Heart
SIS	Segment involved score
TRIPOD	Transparent Reporting of a multivariable prediction model for Individual Prognosis Or Diagnosis

Introduction

Coronary artery disease (CAD) is still the primary cause of death globally [1], despite the substantial improvements in its management in the last years. Nonetheless, early CAD detection and prompt initiation of preventive strategies have been shown to reduce the risk of future cardiovascular events [2]. Therefore, identifying at-risk patients remains one of the priorities for public health [3].

Over the past decade, coronary computed tomography angiography (CCTA) has consolidated its role as a non-invasive imaging modality, which allows for the assessment of the atherosclerotic burden of the overall coronary tree [4]. Beyond the traditional and well-established measurement of diameter stenosis, CCTA provides additional information on plaque location, extent, and composition [5] and on the presence of specific high-risk plaque (HRP) features [6]. Of note, these plaque characteristics were revealed to have superior risk stratification for future cardiovascular events compared to traditional cardiovascular risk factors [7, 8].

Additionally, the accelerated progression of coronary atherosclerosis has been associated with a higher risk of long-term mortality [9]. Although evidence is available concerning the ability of CCTA to assess plaque progression over time [10, 11], no clear recommendations are endorsed by the different scientific societies on the clinical use of repeat CCTA [12–14]. Therefore, this study aimed to develop and validate a practical CCTA risk score to predict medium-term disease progression in a selected population of patients with non-obstructive coronary stenosis, and without HRPs, at baseline CCTA.

Materials and methods

Study design and study population

The PARADIGM (Progression of AtheRosclerotic PlAque Determined by Computed Tomographic Angiography Imaging) registry was a prospective, international, multicenter, observational registry in which 2252 patients at low-to-intermediate risk of CAD were enrolled from 13 sites in 7 countries [15]. Consecutive patients who underwent two repeat, clinically indicated CCTA scans within at least 2 years were prospectively included in the study. Patients with no clinical data available at baseline or follow-up CCTA were excluded. For the present study, additional exclusion criteria were as follows: (1) uninterpretable CCTA either at baseline or follow-up, (2) previous coronary revascularization by either percutaneous coronary intervention (PCI) or coronary artery bypass graft (CABG), (3) presence of at least one obstructive coronary stenosis (≥ 50%) at baseline CCTA, (4) presence of at least one HRP at baseline CCTA, (5) absence of coronary atherosclerosis at baseline CCTA, and (6) PCI and/or CABG between serial CCTAs.

The study protocol complies with the Declaration of Helsinki, and it was approved by the Institutional Ethical Committees of each participating center. All patients gave their written informed consent for the study.

Data collection

Patient demographics, cardiovascular risk factors, laboratory values, and medications were prospectively collected and recorded at the time of baseline and follow-up CCTAs [15].

CCTA analysis and CCTA-derived parameters

All CCTAs were performed on CT scanners with 64-detector rows or higher according to the Society of Cardiovascular Computed Tomography (SCCT) guidelines [16, 17]. Since SCCT guidelines have indicated coronary artery calcium (CAC) scanning as optional at the time of CCTA, CAC imaging was not a requirement for the PARADIGM registry. The median (interquartile range) dose length product (DLP) of baseline CCTA and the cumulative DLP, including baseline and follow-up scans, were 467 (379–569) mGy*cm and 736 (542–1069) mGy*cm, respectively.

All datasets were transferred to an offline workstation in a single core laboratory. Independent, level III experienced readers [18, 19] analyzed the CCTA images blinded to the clinical data. Each coronary segment was inspected for the

presence of coronary atherosclerosis. More specifically, the following characteristics were evaluated:

(a) *Qualitative characteristics*: Coronary plaques were divided into non-calcified, calcified, and partially calcified based on their composition, as previously described [20]. Calcified and partially calcified plaques were grouped in the same category (plaques with calcified component).
(b) *High-risk plaque (HRP)*: HRPs were defined as coronary lesions with ≥ 2 of the following high-risk features: low-attenuation plaque, positive arterial remodelling, spotty calcification, and napkin ring sign [21]. A low-attenuated plaque was defined as the presence of a focal plaque area < 30 Hounsfield unit (HU). Positive arterial remodelling was identified if the lesion diameter divided by reference diameter was ≥ 1.1, and spotty calcification was described as a focal calcification < 3 mm in maximal diameter occupying only one side of the coronary lumen on a cross-sectional view [21]. The napkin-ring sign corresponded to a ring-like peripheral higher attenuation of the non-calcified portion of the coronary plaque [22]. Finally, coronary lesions were evaluated for location at a bifurcation, defined as the presence of a side branch origin within the lesion [23].
(c) *Severity of coronary stenosis*: The degree of stenosis was graded according to SCCT guidelines as follows: (1) none (diameter narrowing = 0%); (2) very mild (< 25%); mild (25–49%); moderate (50–69%); severe (70–99%) and occlusion (100%) [17]. A coronary stenosis was defined as obstructive when diameter narrowing was ≥ 50%. A segment involvement score (SIS) was built as a measure of overall coronary artery plaque distribution. The SIS was calculated as the total number of coronary artery segments exhibiting plaque, irrespective of the degree of luminal stenosis [24].

The most severe coronary stenosis within each patient was selected and included in the analysis, regardless of its location. Imaging datasets of patients included in the PARADIGM registry were also analyzed for quantitative plaque assessment. Since the aim of our study was to develop a practical tool for clinicians which could be implemented easily in the busy clinical routine, we focused the analysis on qualitative and semi-quantitative imaging parameters.

Clinical outcome

The primary outcome of the study was the composite endpoint of (1) development of HRP and obstructive coronary stenosis; (2) development of obstructive coronary stenosis at follow-up CCTA without the development of HRP; and (3) development of HRP at follow-up CCTA without the development of obstructive coronary stenosis.

Statistical analysis

All statistical analyses were performed using STATA version 17 (StataCorp. 2015. *Stata Statistical Software: Release 17*. StataCorp LP). Continuous variables are reported as mean ± standard deviation if normally distributed or as median (interquartile range) if non-normally distributed and compared using the Student unpaired *t*-test or Mann–Whitney *U* test, as appropriate. Categorical variables are presented as frequencies and corresponding percentages and compared using the chi-square test or the Fisher exact test. The risk prediction model was developed according to the TRIPOD (Transparent Reporting of a multivariable prediction model for Individual Prognosis Or Diagnosis) methodology. Briefly, the entire cohort of patients was randomly divided into a derivation cohort, corresponding to approximately two-thirds of the whole population ($n = 370$), and a validation cohort, including the remaining 219 patients. There was no overlap of any patients between the derivation and the validation cohorts. After checking for collinearity, a multivariable logistic regression model was created to evaluate the relationship between potential predictors and disease progression in the derivation cohort. The variables age, sex, the time interval between the two CCTAs, and those showing $p < 0.100$ at the exploratory univariate analysis were included. According to the inclusion criteria, t_0 was set 2 years after the baseline CCTA. To avoid the problem of overfitting and provide meaningful predictors for clinical implementation, only variables with a $p < 0.050$ were retained in the final model by stepwise approach. The Hosmer–Lemeshow test was used to assess the goodness of fit of the final model, and the *C*-statistic was calculated to evaluate the discriminatory power of the model. The *b*-coefficients derived from the final model were divided by the absolute value of the smallest coefficient and rounded to the nearest integer. The calculated weighted coefficients were used to generate a composite risk score. The final model was externally tested in the validation cohort. In addition, patients were classified into low score and high score according to the limits of the interquartile range of the calculated score, rounded to the nearest integer. Values between the 25th and 75th percentiles were used to define the intermediate group. The predicted probability and the rate of disease progression were calculated for each of the three score groups in the development and validation cohorts. All statistical analyses were 2-sided and $p < 0.050$ was considered statistically significant.

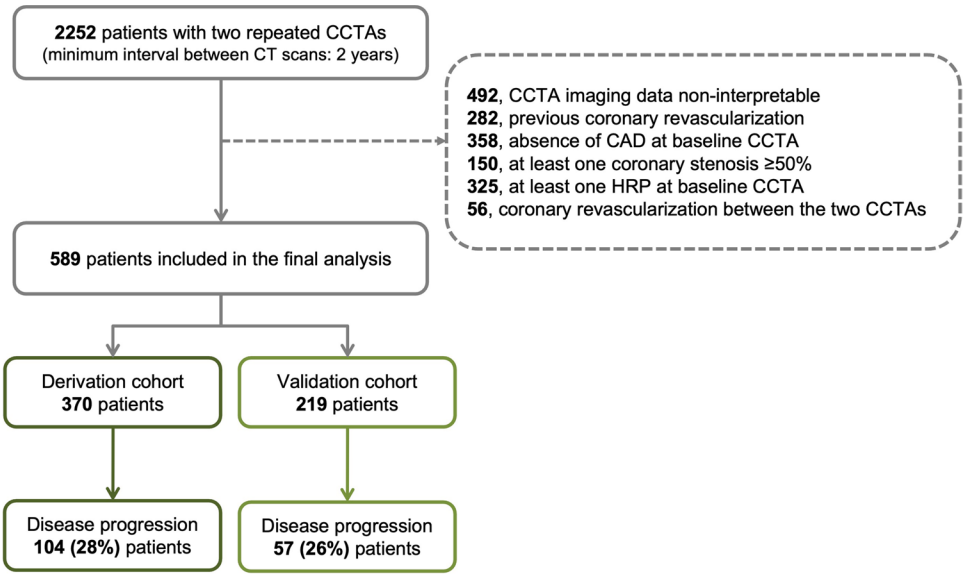

Fig. 1 Inclusion flowchart. *Abbreviations*: CAD, coronary artery disease; CCTA, coronary computed tomography angiography; HRP, high-risk plaque

Abbreviations: CAD, coronary artery disease; CCTA, coronary computed tomography angiography; HRP, high-risk plaque

Results

Study population

From the total population of 2252 patients enrolled in the PARADIGM registry, 492 were excluded because either baseline or follow-up CCTA was not suitable for analysis, 282 due to previous coronary revascularization, 150 due to the presence of obstructive coronary stenosis at baseline CCTA, 325 due to the detection of HRP at baseline CCTA, 358 due to the absence of coronary atherosclerosis at baseline CCTA, and 56 due to coronary revascularization between serial CCTA scans. Therefore, the final population of the study consisted of 589 patients, as reported in the inclusion flowchart in Fig. 1.

The derivation group comprised 370 patients and the validation cohort included 219 patients. Patient demographics, cardiovascular risk factors, laboratory values, medications, and imaging parameters at baseline did not differ significantly between the derivation and validation cohorts, as shown in Table 1S and Table 2S (Online Supplementary Material). There was a comparable rate of disease progression in the two cohorts: 104 (28%) in the derivation group and 57 (26%) in the validation group ($p = 0.584$).

Derivation cohort

The baseline clinical and laboratory characteristics of the derivation cohort are detailed in Table 1. The mean age was 61 ± 8.7 years and 203 (55%) patients were males. A total of 198 patients (54%) had hypertension, 84 (23%) had diabetes, 148 (40%) had hyperlipidemia, and 61 (16%) were active smokers at the time of enrolment. The baseline imaging characteristics are reported in Table 2. The median time interval between the first and the second CCTA was 3.3 years (2.7–4.8). The median SIS was 3 (2–4) and a total of 123 (33%) coronary plaques were identified in the left main (LM) or in the proximal left anterior descending (LAD) coronary artery. Most coronary plaques (76%) were either partially calcified or calcified. Regarding the severity of coronary lesions, 204 (55%) patients presented a coronary stenosis < 25% and the remaining 166 (45%) patients showed a 25–49% coronary stenosis. The prevalence of HRP features at baseline was 79% for positive remodelling, 6% for low attenuation plaque, 5% for spotty calcification, and 72% for bifurcation lesions.

Characteristic of the population according to disease progression in the derivation cohort

The primary endpoint of disease progression occurred in 104 (28%) patients. Specifically, 25 (24%) developed only obstructive CAD, 71 (68%) only HRP, and 8 (8%) both obstructive CAD and HRP. The clinical, laboratory, and imaging characteristics of patients with and without disease progression are reported in Table 1 and Table 2. Patients who experienced disease progression were more likely diabetic compared to patients without the primary endpoint. With regard to imaging parameters, patients with the primary endpoint had a higher SIS, presented a higher rate of coronary stenosis between 25 and 49%, and had HRP features more frequently at baseline.

Model development

The exploratory univariable analysis performed in the derivation group is presented in Table 3S (Online Supplementary

Table 1 Baseline clinical and laboratory characteristics in patients with versus without disease progression in the derivation group

	All ($n=370$)	Disease progression ($n=104$)	No disease progression ($n=266$)	p
Age, yrs	61 ± 8.7	61 ± 7.7	61 ± 9.1	0.892
Sex (male)	203 (55)	63 (61)	140 (53)	0.167
Cardiovascular risk factors				
Body mass index, kg/m^2	26 ± 3.7	26 ± 3.6	26 ± 3.7	0.432
Hypertension	198 (54)	55 (53)	143 (54)	0.658
Diabetes mellitus	84 (23)	32 (31)	52 (20)	0.058
Hyperlipidemia	148 (40)	38 (37)	110 (41)	0.618
Family history of CAD	111 (30)	34 (33)	77 (29)	0.480
Current smoker	61 (16)	22 (21)	39 (15)	0.131
Symptoms				
No symptoms	65 (18)	16 (15)	49 (18)	0.777
Dyspnea	24 (6)	6 (6)	18 (7)	0.924
Non-cardiac chest pain	38 (10)	8 (8)	30 (11)	0.726
Atypical chest pain	248 (67)	74 (71)	174 (65)	0.573
Typical chest pain	10 (3)	2 (2)	8 (3)	0.887
Baseline lipid profile				
Total cholesterol, mg/dl	191 (163–215)	193 (163–229)	189 (164–212)	0.171
Low-density lipoprotein, mg/dl	113 (91–138)	114 (91–151)	113 (91–134)	0.360
High-density lipoprotein, mg/dl	50 (42–60)	51 (41–60)	50 (43–59)	0.948
Triglycerides, mg/dl	117 (87–177)	132 (98–177)	113 (85–176)	0.118
Medications				
Statins	147 (40)	44 (42)	103 (39)	0.670
Antiplatelet	136 (37)	44 (42)	92 (35)	0.065
Beta-blockers	98 (26)	27 (26)	71 (27)	0.379
Antidiabetic	51 (14)	18 (17)	33 (12)	0.219

Continuous variables are reported as mean ± standard deviation or median (interquartile range), as appropriate, and compared using the Student unpaired *t* test or the Mann–Whitney *U* test. Categorical variables are presented as frequencies (percent) and compared using the chi-square test or Fisher exact test

Abbreviation: *CAD* coronary artery disease

Material). The following variables were used to create the multivariable model: age, sex, time interval between the two CCTAs, diabetes mellitus, number of plaques with positive remodelling, number of low attenuation plaques, number of spotty calcifications, number of bifurcation lesions, SIS, and stenosis severity. The final model included only predictors with $p<0.050$: time interval between the two CCTAs, number of low attenuation plaques, number of spotty calcifications, number of bifurcation lesions, and stenosis severity. The estimates of the *b*-coefficients, odds ratios and corresponding 95% confidence interval from the initial and final multivariable logistic regression models are presented in Table 3. The final model had good discrimination with a *C*-statistic of 0.732 (0.676–0.788) and was well calibrated (Hosmer–Lemeshow χ^2, $p=0.216$ and Pearson χ^2, $p=0.472$).

From the weight of regression coefficients, we derived the following risk score system: score = 1 (time interval between CCTAs, years) + 7 (number of low attenuation plaques) + 8 (number of plaques with spotty calcification) + 2 (number of bifurcation lesions) + 5 (if coronary stenosis 1–24%) or 10 (if coronary stenosis 25–49%). According to the predicted risk score, patients were divided into three groups: low (score ≤ 8, $n=104$), intermediate (score: 9–14, $n=178$), and high (score ≥ 15 $n=88$) score. The rates of disease progression by the three score categories are shown in Fig. 2. The mean probabilities of developing disease progression were 11 ± 2.0% in the low score group, 26 ± 6.6% in the intermediate score group, and 53 ± 13% in the high score group.

Model performance in the validation cohort

The performance of the model in the validation group was satisfactory with a *C*-index of 0.668 (0.583–0.752). The model showed good calibration (Hosmer–Lemeshow χ^2, $p=0.824$ and Pearson χ^2, $p=0.179$). The performance of the risk score derived from the weighted coefficients in the derivation and validation groups was comparable ($p=0.217$), as shown in Fig. 3. According to the risk score, 71 (32%) patients were in the low score group, 100 (46%) in

Table 2 Baseline CCTA characteristics in patients with versus without disease progression in the derivation group

	All ($n=370$)	Disease progression ($n=104$)	No disease progression ($n=266$)	p
CCTA scan interval, yrs	3.3 (2.7–4.8)	3.7 (2.9–4.7)	3.3 (2.6–4.8)	0.096
Agatston calcium score *	31 (0.0–101)	64 (31–143)	14 (0.0–75)	<0.001
Calcified plaques	281 (76)	83 (80)	198 (74)	0.277
LM/LAD location	123 (33)	34 (33)	89 (33)	0.888
Positive arterial remodelling ≥ 1	294 (79)	88 (85)	206 (77)	0.125
Positive arterial remodelling, range	0–8	0–8	0–8	-
Low attenuation plaque ≥ 1	22 (6)	12 (12)	10 (4)	0.007
Low attenuation plaque, range	0–2	0–2	0–1	-
Spotty calcification ≥ 1	19 (5)	11 (11)	8 (3)	0.007
Spotty calcification, range	0–1	0–1	0–1	-
Bifurcation lesion ≥ 1	268 (72)	90 (87)	178 (67)	<0.001
Bifurcation lesion, range	0–7	0–7	0–6	-
Stenosis 1–24%	204 (55)	39 (38)	165 (62)	<0.001
Stenosis 25–49%	166 (45)	65 (63)	101 (38)	
Segment involvement score, *n*	3 (2–4)	3 (2–5)	2 (1–4)	0.002

Continuous variables are reported as median (interquartile range) and compared using the Mann–Whitney *U* test. Categorical variables are presented as frequencies (percent) and compared using the chi-square test or Fisher exact test

*The Agatston calcium score was available only in 185 patients; of those, 56 (30%) showed disease progression

Abbreviations: *CCTA* coronary computed angiography tomography, *LAD* left anterior descending artery, *LM* left main

the intermediate score group, and 48 (22%) patients in the high score group. The rates of disease progression in each of the 3 score groups in the validation set were comparable with those in the groups of the development set, as shown in Fig. 2.

A graphical representation of the new CCTA-based risk score is presented in Fig. 4.

Discussion

In the current study, we developed a simple and practical score to predict disease progression from a single-point CCTA in a population of patients at low-to-intermediate risk of CAD. The model was derived using data from the large and well-characterized PARADIGM population, which included patients who underwent two repeat, clinically indicated CCTAs within a time interval of at least 2 years. The main findings of the study were as follows: (1) the rate of disease progression in the derivation cohort was 28%; (2) the time interval between the two CCTAs, the presence of residual high-risk features (low attenuation plaque, spotty calcification, and bifurcation lesions), and the severity of non-obstructive stenosis were independent predictors of disease progression; and (3) the model was able to discriminate between patients at low and high risk of disease progression, as documented by the *C*-statistic in both derivation and validation cohorts.

Our study aimed to assess the development of either obstructive stenosis or HRP at follow-up in a selected cohort of patients with mild CAD at baseline CCTA. Combining two morphological parameters as endpoint is justified because they are both associated with adverse cardiovascular outcomes [24, 25]. In addition, both findings can change patient management in terms of downstream stress imaging test and medical therapy. Indeed, atherosclerosis is a dynamic process that the implementation of lipid-lowering therapy can modify. In a sub-analysis of the PARADIGM registry, Lee et al [26] demonstrated that statin-taking patients presented a slower annualized progression of plaque volume and a lower annualized incidence of HRP than statin-naive patients. This supports that patients at increased risk of disease progression would benefit from aggressive risk reduction therapies.

Our final model included only five significant predictors that can be easily used in a busy clinical setting. *Time interval between the CCTA scans.* In line with previous non-invasive [27] and invasive [28] studies, we found that the time interval between the two CCTAs is a predictor of disease progression. However, the most appropriate and clinically relevant interval needs to be estimated in larger populations combining the information on disease progression, effect of medications, and cardiovascular events.

Non-obstructive CAD. Looking at the imaging parameters, interesting data have emerged about the impact of the severity of non-obstructive CAD on disease progression. Our work expanded the results of previous prognostic

Table 3 Multivariable logistic regression models for prediction of disease progression in the derivation group

	Initial multivariable model			Final multivariable model			
	B	OR (95% CI)	*p*	*B*	OR (95% CI)	*p*	Score
Age	–0.014	0.99 (0.96–1.02)	0.340				
Sex	–0.347	0.71 (0.42–1.19)	0.191				
CCTA scan interval, yrs	0.186	1.20 (1.02–1.42)	0.028	0.187	1.21 (1.02–1.42)	0.026	1
Diabetes mellitus	0.414	1.51 (0.85–2.69)	0.160				
Positive arterial remodelling, n	0.100	1.11 (0.87–1.41)	0.415				
Low attenuation plaque, n	1.302	3.68 (1.40–9.66)	0.008	1.317	3.73 (1.46–9.52)	0.006	7
Spotty calcification, n	1.608	4.99 (1.77–14.04)	0.002	1.525	4.59 (1.69–12.48)	0.003	8
Bifurcation lesion, n	0.483	1.62 (1.21–2.16)	0.001	0.384	1.47 (1.17–1.84)	0.001	2
Stenosis 25–49% vs. 1–24%	1.052	2.86 (1.64–5.01)	<0.001	0.995	2.71 (1.62–4.50)	<0.001	5 (1–24%) 10 (25–49%)
Segment involvement score	–0.135	0.87 (0.71–1.07)	0.198				

Abbreviation: *CCTA* coronary computed angiography tomography

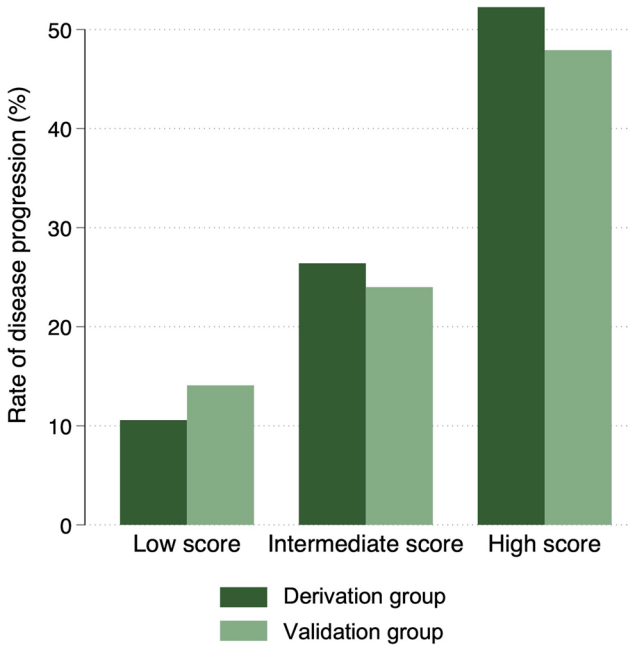

Fig. 2 Rate of disease progression by the 3 score groups in the development and validation groups. The rate of disease progression by the three score groups was similar in the derivation and validation groups

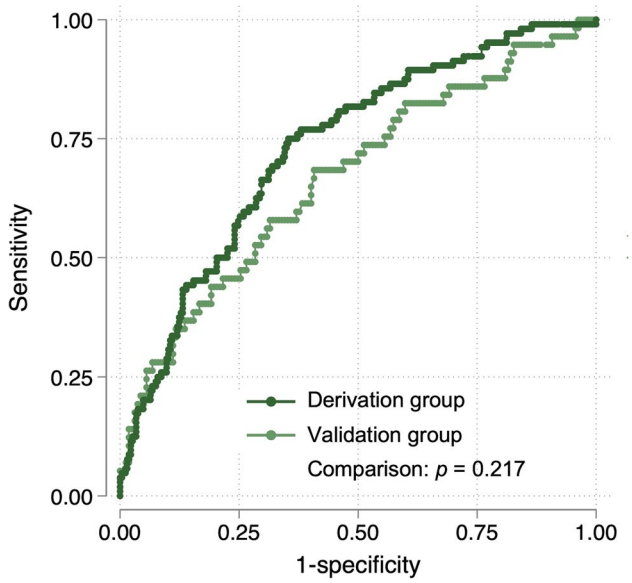

Fig. 3 Comparison of model performance in the derivation and validation groups. Receiver operating characteristic (ROC) curves for the disease progression showed comparable performance of the prediction model in the development and validation groups ($p = 0.217$). The ROCs were built using the predicted probability derived from the final model. The correlation between the predicted probability and the calculated score was 0.990 ($p < 0.001$) in the derivation group and 0.988 (p-value < 0.001) in the validation cohort

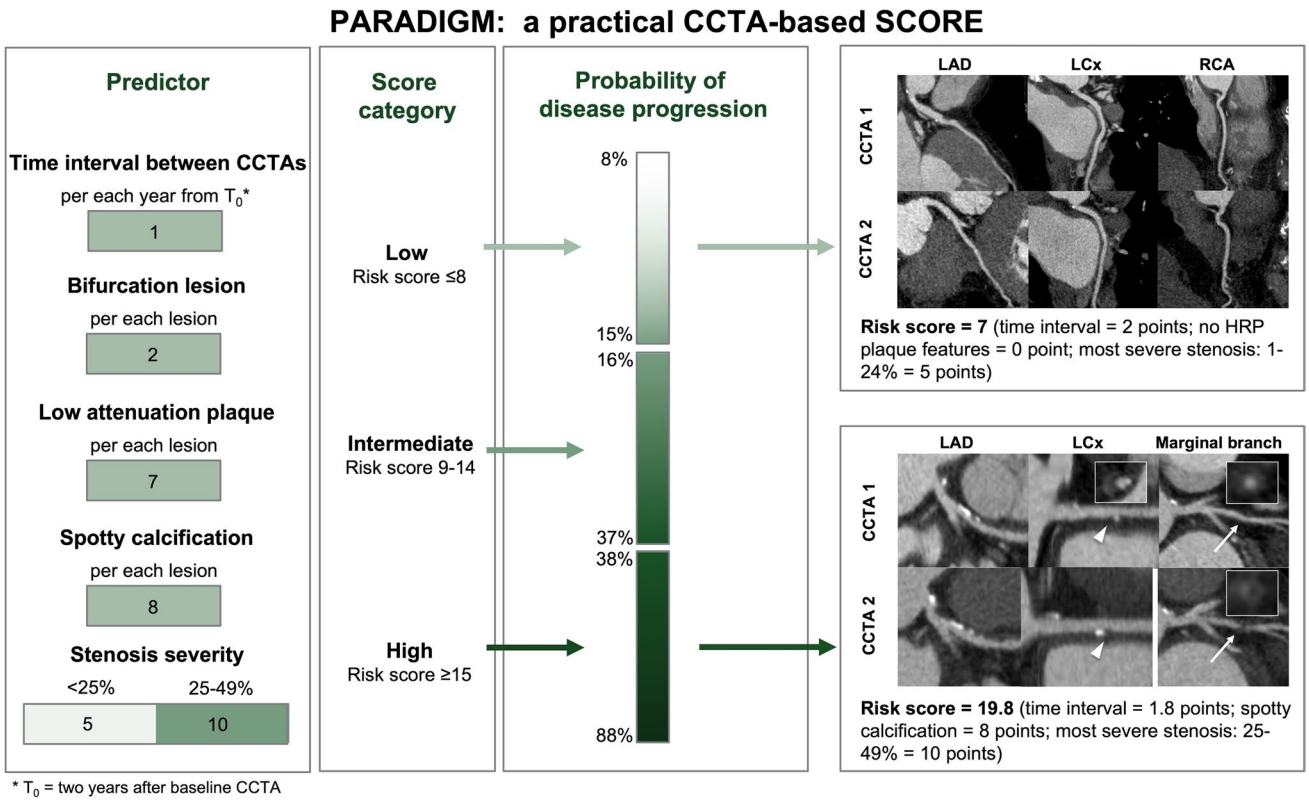

Fig. 4 Graphical illustration of the new CCTA-based risk score. The points attributed to each predictor of the model are provided. Adding the points obtained from each predictor yields the total score and the corresponding probability of disease progression. *Representative images from a patient with a low score*. A 67-year-old man, known for hypertension and a family history of CAD, developed atypical chest pain. He subsequently performed CCTA (CCTA 1, curved MPRs), showing minimal, mostly calcified disease of LM, proximal LAD, and proximal RCA, and no disease of LCx. After 48 months, he complained of several episodes of atypical chest pain, and he underwent a follow-up CCTA (CCTA 2, curved MPRs). Based on the predictors (time interval = 2 points; no HRP plaque features = 0; most severe stenosis: 1–24% = 5 points), the risk score was 7. The follow-up CCTA showed disease stability. *Representative images from a patient with a high score*. A 70-year-old man smoker, known for hypertension and dyslipidemia, underwent CCTA due to atypical chest pain. CCTA images (CCTA 1, curved MPRs and cross-sectional images) showed minimal-to-mild, mostly calcified disease of LM and proximal LAD. A spotty calcification was detected in the proximal LCx (arrowhead). A non-calcified plaque causing a 30% lumen reduction was detected in the main obtuse marginal branch (arrow). No disease was identified on RCA. After 46 months, the patient developed effort angina and underwent a follow-up CCTA (CCTA 2, curved MPRs, and cross-sectional image). Based on the predictors (time interval = 1.8 point; presence of spotty calcification in the proximal LCx = 8; most severe stenosis: 25–49% = 10 points), the risk score was 19.8. The follow-up CCTA showed significant disease progression at the level of the main obtuse marginal branch with associated development of HRP features (arrow). *Abbreviations*: CAD, coronary artery disease; CCTA, coronary computed tomography angiography; HRP, high-risk plaque; LAD, left anterior descending; LM, left main; LCx, left circumflex; MRP, multiplanar reconstruction; RCA, right coronary artery

studies [29, 30], which demonstrated that non-obstructive CAD is associated with a higher rate of cardiovascular events compared to no CAD. Like findings previously reported by Kumamaru et al [27], we also found that stenoses between 25 and 49% are associated with a significantly increased risk of developing disease progression compared to those between 1 and 24%. Historically, the identification of obstructive CAD has been the primary focus in the management of patients with stable angina. Nevertheless, a unique advantage of CCTA is the ability to image and quantify non-obstructive CAD, a stage of the disease which is often misdiagnosed by functional testing. This aspect is critical since approximately half of the myocardial infarctions in the Scottish Computed Tomography of the Heart (SCOT-HEART) population occurred in patients with non-obstructive CAD [2]. As such, the recently released international guidelines propose CCTA as a reasonable tool in patients with known non-obstructive CAD to determine atherosclerotic plaque burden and guide therapeutic decision-making [14].

HRP features. Our results confirmed the findings of a recent paper from von Rosendael et al showing that baseline plaque burden and the number of HRP features at baseline are the strongest determinants of atherosclerosis progression [31]. Data from several CCTA studies have reported that HRP features are strongly associated with a higher risk

of future acute coronary syndrome [32, 33]. In addition, in a sub-study of the Prospective Multicenter Imaging Study for Evaluation of Chest Pain (PROMISE) trial, the presence of HRP in patients with non-obstructive CAD doubled the incidence of major adverse cardiovascular events [25]. Nevertheless, the prevalence of single HRP features on CCTA is usually high [33]. Such lesions can heal spontaneously or thanks to statin treatment, thus reducing the positive predictive value of CCTA for identifying patients at risk for future events [33]. Since combining multiple HRP features has been shown to improve risk prediction [34], we used a stringent definition of HRP (≥ 2 high-risk plaque features) as an exclusion criterion for our study. Still, in our analysis, spotty calcification and low attenuation plaque, as single plaque features, were identified as independent predictors of disease progression. This could be explained by the fact that subjects with a tendency to develop such lesions will present other plaques with HRP features in other sites of the coronary tree in a dynamic formation and healing process, remaining at increased risk for future events [33]. Bifurcation location has also been associated with disease progression, likely due to its relationship with local hemodynamic factors, such as wall shear stress, that facilitate plaque formation and development of HRP features [23].

Given this context, this new CCTA-based risk score may have two practical implications in the management of patients with CAD. The first one is the identification of those subjects with prior evidence of non-obstructive CAD on CCTA who may benefit from a repeat scan in the medium term. If the recommendation of repeat CCTA should be limited to patients with high-risk score, or should be extended to the intermediate-risk category, it needs further validation in larger prospective cohorts. This decision should also consider that CCTA has been challenged during past years due to the increased lifetime attributable risk estimates of developing cancer associated with its radiation exposure [35]. Although radiation dose has progressively decreased over the past years resulting in scans of ≤ 1 mSv with the latest CT technology [36], a comprehensive risk–benefit assessment remains mandatory for the evaluation of asymptomatic patients and follow-up studies.

The second implication is the individualized tailoring of the intensity of medical treatment in secondary prevention. The results of our study lay the groundwork for using CCTA, in combination with clinical cardiovascular risk factors, as a supporting tool for the decision of initiating or intensifying preventive strategies in symptomatic patients according to the risk of disease progression. This statement is supported by the findings of a recently published study by Mortensen et al [37]. In a large population of 20,241 symptomatic patients, the authors confirmed that the severity of CAD was strongly associated with the rate of atherosclerotic cardiovascular disease events. Even more important, adding the information of the extent of CAD burden on CCTA to the level of LDL-C helped identify patients who were likely to benefit most from intensive lipid-lowering therapy, thus achieving the guidelines treatment targets.

This study has several limitations. First, this is a registry study in which patients underwent a second CCTA because of recurrent symptoms, thus introducing a selection bias. Second, excluding all patients with either no signs of CAD or obstructive CAD at baseline limits the potential implementation of this CCTA-based risk score only to patients with non-obstructive coronary plaques at baseline. Nevertheless, disease progression in patients with a normal CCTA is likely to be a rare event. Indeed, as previously shown, the annualized event rate in patients with normal CCTA is 0.2% compared to 0.8% of those with non-obstructive CAD [30]. On the other hand, patients with obstructive CAD at baseline are likely to undergo additional downstream testing for myocardial ischemia or invasive coronary angiography for coronary revascularization. Third, only qualitative and semi-quantitative CCTA-derived parameters were analyzed as potential independent predictors for the CCTA-based score. Despite the percentage atheroma volume at baseline was previously identified as an independent predictor of accelerated disease progression [26], quantitative plaque assessment is still time-consuming, limiting its use to a research environment [38]. Further development of artificial intelligence methods might help fully automated segmentation of the coronary arteries, facilitating the implementation of quantitative plaque analysis in the clinical routine. Fourth, calcium score values and intensity of medical therapy after the baseline CCTA were not considered. In particular, calcium score values were available only for 288 patients, precluding the investigation of this parameter as a potential predictor of disease progression. Since the median value of calcium score was also low in patients with disease progression, the developed score remains to be validated in patients with moderate or high calcium. Finally, the size of the validation cohort was relatively small likely leading to the limited performance of the score. Further prospective studies involving larger populations are warranted to confirm the performance of this newly developed score before its potential implementation in the daily clinical routine.

Conclusions

The new CCTA-based risk score is a simple and practical tool which has the potential to predict mid-term coronary artery disease progression in patients with non-obstructive CAD. We believe that this may promote the clinical

management of CAD patients in terms of timing of imaging follow-up and related therapeutic strategies.

Supplementary information The online version contains supplementary material available at https://doi.org/10.1007/s00330-023-09880-x.

Funding Partial funding was provided by a gift from the Dalio Foundation (New York, NY). This work was also supported by the Leading Foreign Research Institute Recruitment Program through the National Research Foundation funded by the Ministry of Science and Information and Communications Technology of Korea (Grant no. 2012027176).

Declarations

Guarantor The scientific guarantor of this publication is Gianluca Pontone.

Conflict of interest The authors of this manuscript declare the following relationships:
- Dr. Chinnaiyan is a (non-compensated) medical advisor for Heartflow, Inc.
- Dr. Shaw serves on the scientific advisory board for Covanos, Inc.
- Dr. Pontone receives Speaker honorarium and/or research grant from GE Healthcare and BRACCO, Bhoeringer.
- Dr. Min was involved in this registry prior to leaving Weill Cornell Medical College. He currently is an employee of Cleerly, Inc.
- All other authors do not report any conflicts.

Statistics and biometry One of the authors has significant statistical expertise.

Informed consent Written informed consent was obtained from all subjects (patients) in this study.

Ethical approval Institutional Review Board approval was obtained.

Study subjects or cohorts overlap The PARADIGM (Progression of AtheRosclerotic PlAque Determined by Computed Tomographic Angiography Imaging) registry was a prospective, international, multicenter, observational registry in which patients were enrolled from 13 sites in 7 countries. So far, several research studies with different research aims have been published.

Methodology
- prospective
- observational
- multicenter study

References

1. Dagenais GR, Leong DP, Rangarajan S et al (2020) Variations in common diseases, hospital admissions, and deaths in middle-aged adults in 21 countries from five continents (PURE): a prospective cohort study. Lancet 395:785–794
2. Investigators S-H, Newby DE, Adamson PD et al (2018) Coronary CT angiography and 5-year risk of myocardial infarction. N Engl J Med 379:924–933
3. Franco M, Cooper RS, Bilal U, Fuster V (2011) Challenges and opportunities for cardiovascular disease prevention. Am J Med 124:95–102
4. Al-Mallah MH, Qureshi W, Lin FY et al (2014) Does coronary CT angiography improve risk stratification over coronary calcium scoring in symptomatic patients with suspected coronary artery disease? Results from the prospective multicenter international CONFIRM registry. Eur Heart J Cardiovasc Imaging 15:267–274
5. Hoffmann U, Moselewski F, Nieman K et al (2006) Noninvasive assessment of plaque morphology and composition in culprit and stable lesions in acute coronary syndrome and stable lesions in stable angina by multidetector computed tomography. J Am Coll Cardiol 47:1655–1662
6. Motoyama S, Ito H, Sarai M et al (2015) Plaque characterization by coronary computed tomography angiography and the likelihood of acute coronary events in mid-term follow-up. J Am Coll Cardiol 66:337–346
7. Deseive S, Kupke M, Straub R et al (2020) Quantified coronary total plaque volume from computed tomography angiography provides superior 10-year risk stratification. Eur Heart J Cardiovasc Imaging 22:314–321. https://doi.org/10.1093/ehjci/jeaa228
8. van Rosendael AR, Shaw LJ, Xie JX et al (2019) Superior risk stratification with coronary computed tomography angiography using a comprehensive atherosclerotic risk score. JACC Cardiovasc Imaging 12:1987–1997
9. Ndrepepa G, Iijima R, Kufner S et al (2016) Association of progression or regression of coronary artery atherosclerosis with long-term prognosis. Am Heart J 177:9–16
10. Lee SE, Sung JM, Rizvi A et al (2018) Quantification of coronary atherosclerosis in the assessment of coronary artery disease. Circ Cardiovasc Imaging 11:e007562
11. Papadopoulou SL, Neefjes LA, Garcia-Garcia HM et al (2012) Natural history of coronary atherosclerosis by multislice computed tomography. JACC Cardiovasc Imaging 5:S28-37
12. Pontone G, Rossi A, Guglielmo M et al (2022) Clinical applications of cardiac computed tomography: a consensus paper of the European Association of Cardiovascular Imaging-part II. Eur Heart J Cardiovasc Imaging 23:e136–e161
13. Pontone G, Rossi A, Guglielmo M et al (2022) Clinical applications of cardiac computed tomography: a consensus paper of the European Association of Cardiovascular Imaging-part I. Eur Heart J Cardiovasc Imaging 23:299–314
14. Gulati M, Levy PD, Mukherjee D et al (2021) 2021 AHA/ACC/ASE/CHEST/SAEM/SCCT/SCMR Guideline for the Evaluation and Diagnosis of Chest Pain: A Report of the American College of Cardiology/American Heart Association Joint Committee on Clinical Practice Guidelines. Circulation 144:e368–e454
15. Lee SE, Chang HJ, Rizvi A et al (2016) Rationale and design of the Progression of AtheRosclerotic PlAque DetermIned by Computed TomoGraphic Angiography IMaging (PARADIGM) registry: a comprehensive exploration of plaque progression and its impact on clinical outcomes from a multicenter serial coronary computed tomographic angiography study. Am Heart J 182:72–79
16. Abbara S, Blanke P, Maroules CD et al (2016) SCCT guidelines for the performance and acquisition of coronary computed tomographic angiography: a report of the society of Cardiovascular Computed Tomography Guidelines Committee: Endorsed by the North American Society for Cardiovascular Imaging (NASCI). J Cardiovasc Comput Tomogr 10:435–449
17. Leipsic J, Abbara S, Achenbach S et al (2014) SCCT guidelines for the interpretation and reporting of coronary CT angiography: a report of the Society of Cardiovascular Computed Tomography Guidelines Committee. J Cardiovasc Comput Tomogr 8:342–358
18. Choi AD, Thomas DM, Lee J et al (2021) 2020 SCCT Guideline for Training Cardiology and Radiology Trainees as Independent Practitioners (Level II) and Advanced Practitioners (Level III) in Cardiovascular Computed Tomography: a statement from the Society of Cardiovascular Computed Tomography. J Cardiovasc Comput Tomogr 15:2–15

19. Pontone G, Moharem-Elgamal S, Maurovich-Horvat P et al (2018) Training in cardiac computed tomography: EACVI certification process. Eur Heart J Cardiovasc Imaging 19:123–126
20. Hadamitzky M, Achenbach S, Al-Mallah M et al (2013) Optimized prognostic score for coronary computed tomographic angiography: results from the CONFIRM registry (COronary CT Angiography EvaluatioN For Clinical Outcomes: An InteRnational Multicenter Registry). J Am Coll Cardiol 62:468–476
21. Puchner SB, Liu T, Mayrhofer T et al (2014) High-risk plaque detected on coronary CT angiography predicts acute coronary syndromes independent of significant stenosis in acute chest pain: results from the ROMICAT-II trial. J Am Coll Cardiol 64:684–692
22. Maurovich-Horvat P, Hoffmann U, Vorpahl M, Nakano M, Virmani R, Alkadhi H (2010) The napkin-ring sign: CT signature of high-risk coronary plaques? JACC Cardiovasc Imaging 3:440–444
23. Han D, Lin A, Kuronuma K et al (2022) Association of plaque location and vessel geometry determined by coronary computed tomographic angiography with future acute coronary syndrome-causing culprit lesions. JAMA Cardiol 7:309–319
24. Min JK, Shaw LJ, Devereux RB et al (2007) Prognostic value of multidetector coronary computed tomographic angiography for prediction of all-cause mortality. J Am Coll Cardiol 50:1161–1170
25. Ferencik M, Mayrhofer T, Bittner DO et al (2018) Use of high-risk coronary atherosclerotic plaque detection for risk stratification of patients with stable chest pain: a secondary analysis of the PROMISE Randomized Clinical Trial. JAMA Cardiol 3:144–152
26. Lee SE, Sung JM, Andreini D et al (2020) Differences in progression to obstructive lesions per high-risk plaque features and plaque volumes with CCTA. JACC Cardiovasc Imaging 13:1409–1417
27. Kumamaru KK, Kondo T, Kumamaru H, Amanuma M, George E, Rybicki FJ (2014) Repeat coronary computed tomographic angiography in patients with a prior scan excluding significant stenosis. Circ Cardiovasc Imaging 7:788–795
28. Moise A, Theroux P, Taeymans Y et al (1984) Clinical and angiographic factors associated with progression of coronary artery disease. J Am Coll Cardiol 3:659–667
29. Bittencourt MS, Hulten E, Ghoshhajra B et al (2014) Prognostic value of nonobstructive and obstructive coronary artery disease detected by coronary computed tomography angiography to identify cardiovascular events. Circ Cardiovasc Imaging 7:282–291
30. Hadamitzky M, Taubert S, Deseive S et al (2013) Prognostic value of coronary computed tomography angiography during 5 years of follow-up in patients with suspected coronary artery disease. Eur Heart J 34:3277–3285
31. van Rosendael SE, van den Hoogen IJ, Lin FY et al (2022) Clinical and coronary plaque predictors of atherosclerotic nonresponse to statin therapy. JACC Cardiovasc Imaging. https://doi.org/10.1016/j.jcmg.2022.10.017
32. Thomsen C, Abdulla J (2016) Characteristics of high-risk coronary plaques identified by computed tomographic angiography and associated prognosis: a systematic review and meta-analysis. Eur Heart J Cardiovasc Imaging 17:120–129
33. Dweck MR, Maurovich-Horvat P, Leiner T et al (2020) Contemporary rationale for non-invasive imaging of adverse coronary plaque features to identify the vulnerable patient: a Position Paper from the European Society of Cardiology Working Group on Atherosclerosis and Vascular Biology and the European Association of Cardiovascular Imaging. Eur Heart J Cardiovasc Imaging 21:1177–1183
34. Cury RC, Leipsic J, Abbara S et al (2022) CAD-RADS 2.0 - 2022 Coronary Artery Disease-Reporting and Data System: An Expert Consensus Document of the Society of Cardiovascular Computed Tomography (SCCT), the American College of Cardiology (ACC), the American College of Radiology (ACR), and the North America Society of Cardiovascular Imaging (NASCI). JACC Cardiovasc Imaging 15:1974–2001
35. Einstein AJ, Moser KW, Thompson RC, Cerqueira MD, Henzlova MJ (2007) Radiation dose to patients from cardiac diagnostic imaging. Circulation 116:1290–1305
36. Stocker TJ, Deseive S, Leipsic J et al (2018) Reduction in radiation exposure in cardiovascular computed tomography imaging: results from the PROspective multicenter registry on radiaTion dose Estimates of cardiac CT angIOgraphy iN daily practice in 2017 (PROTECTION VI). Eur Heart J 39:3715–3723
37. Mortensen MB, Steffensen FH, Botker HE et al (2020) CAD Severity on Cardiac CTA Identifies Patients With Most Benefit of Treating LDL Cholesterol to ACC/AHA and ESC/EAS Targets. JACC Cardiovasc Imaging 13(9):1961–1972. https://doi.org/10.1016/j.jcmg.2020.03.017
38. Shaw LJ, Blankstein R, Bax JJ et al (2021) Society of Cardiovascular Computed Tomography / North American Society of Cardiovascular Imaging - Expert Consensus Document on Coronary CT Imaging of Atherosclerotic Plaque. J Cardiovasc Comput Tomogr 15:93–109

Publisher's note Springer Nature remains neutral with regard to jurisdictional claims in published maps and institutional affiliations.

Springer Nature or its licensor (e.g. a society or other partner) holds exclusive rights to this article under a publishing agreement with the author(s) or other rightsholder(s); author self-archiving of the accepted manuscript version of this article is solely governed by the terms of such publishing agreement and applicable law.

Authors and Affiliations

Gianluca Pontone[1,2] · Alexia Rossi[3,4] · Andrea Baggiano[1] · Daniele Andreini[1,5] · Edoardo Conte[1] · Laura Fusini[1] · Chaterine Gebhard[3,4] · Mark G. Rabbat[6] · Andrea Guaricci[7] · Marco Guglielmo[1] · Giuseppe Muscogiuri[1] · Saima Mushtaq[1] · Mouaz H. Al-Mallah[8] · Daniel S. Berman[9] · Matthew J. Budoff[10] · Filippo Cademartiri[11] · Kavitha Chinnaiyan[12] · Jung Hyun Choi[13] · Eun Ju Chun[14] · Pedro de Araújo Gonçalves[15,16] · Ilan Gottlieb[17] · Martin Hadamitzky[18] · Yong Jin Kim[19] · Byoung Kwon Lee[20] · Sang-Eun Lee[21,22] · Erica Maffei[23] · Hugo Marques[15] · Habib Samady[24] · Sanghoon Shin[21] · Ji Min Sung[22,25] · Alexander van Rosendael[26] · Renu Virmani[27] · Jeroen J. Bax[28,29] · Jonathon A. Leipsic[30] · Fay Y. Lin[26] · James K. Min[31] · Jagat Narula[32] · Leslee J. Shaw[26] · Hyuk-Jae Chang[22,25]

✉ Gianluca Pontone
gianluca.pontone@ccfm.it

1 Department of Perioperative Cardiology and Cardiovascular Imaging, Centro Cardiologico Monzino IRCCS, Milan, Italy

2 Department of Biomedical, Surgical and Dental Sciences, University of Milan, Milan, Italy

3 Department of Nuclear Medicine, University Hospital Zurich, Zurich, Switzerland

4 Center for Molecular Cardiology, University of Zurich, Zurich, Switzerland

5 Department of Biomedical and Clinical Sciences, University of Milan, Milan, Italy

6 Division of Cardiology, Loyola University Chicago, Edward Hines Jr. VA Hospital, Hines, Chicago, IL, USA

7 Department of Emergency and Organ Transplantation, Institute of Cardiovascular Disease, University Hospital Policlinico of Bari, Bari, Italy

8 Houston Methodist DeBakey Heart & Vascular Center, Houston Methodist Hospital, Houston, TX, USA

9 Department of Imaging and Medicine, Cedars Sinai Medical Center, Los Angeles, CA, USA

10 Department of Medicine, Lundquist Institute at Harbor UCLA Medical Center, Torrance, CA, USA

11 Cardiovascular Imaging Center, SDN IRCCS, Naples, Italy

12 Department of Cardiology, William Beaumont Hospital, Royal Oak, MI, USA

13 Busan University Hospital, Busan, South Korea

14 Seoul National University Bundang Hospital, Sungnam, South Korea

15 Unit of Cardiovascular Imaging, UNICA, Hospital da Luz, Lisbon, Portugal

16 NOVA Medical School, Lisbon, Portugal

17 Department of Radiology, Casa de Saude São Jose, Rio de Janeiro, Brazil

18 Department of Radiology and Nuclear Medicine, German Heart Center Munich, Munich, Germany

19 Department of Internal Medicine, Seoul National University College of Medicine, Seoul National University Hospital, Cardiovascular Center, Seoul, South Korea

20 Gangnam Severance Hospital, Yonsei University College of Medicine, Seoul, South Korea

21 Division of Cardiology, Department of Internal Medicine, Ewha Womans University Seoul Hospital, Seoul, South Korea

22 Yonsei-Cedars-Sinai Integrative Cardiovascular Imaging Research Center, Yonsei University College of Medicine, Yonsei University Health System, Seoul, South Korea

23 Department of Radiology, Area Vasta 1/ASUR, Marche, Urbino, Italy

24 Division of Cardiology, Emory University School of Medicine, Atlanta, GA, USA

25 Division of Cardiology, Severance Cardiovascular Hospital, Yonsei University College of Medicine, Yonsei University Health System, Seoul, South Korea

26 Department of Radiology, New York-Presbyterian Hospital and Weill Cornell Medicine, New York, NY, USA

27 Department of Pathology, CVPath Institute, Gaithersburg, MD, USA

28 Department of Cardiology, Leiden University Medical Center, Leiden, The Netherlands

29 Turku Heart Center, University of Turku, Turku University Hospital, Turku, Finland

30 Department of Medicine and Radiology, University of British Columbia, Vancouver, BC, Canada

31 Cleerly, Inc, New York, NY, USA

32 Icahn School of Medicine at Mount Sinai, Mount Sinai Heart, Zena and Michael A. Wiener Cardiovascular Institute, and Marie-Josée and Henry R. Kravis Center for Cardiovascular Health, New York, NY, USA